

Impact of Mitochondrion-Targeting Group on the Reactivity and Cytostatic Pathway of Platinum(IV) Complexes

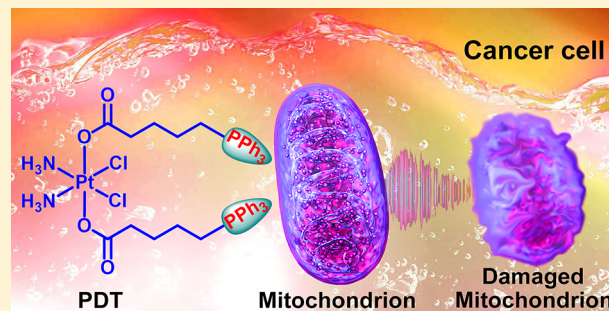
Suxing Jin,[†] Yigang Hao,[‡] Zhenzhu Zhu,^{*,†} Nafees Muhammad,[‡] Zhenqin Zhang,[‡] Kun Wang,[‡] Yan Guo,[‡] Zijian Guo,^{*,‡} and Xiaoyong Wang^{*,†}

[†]State Key Laboratory of Pharmaceutical Biotechnology, School of Life Sciences and [‡]State Key Laboratory of Coordination Chemistry, School of Chemistry and Chemical Engineering, Nanjing University, Nanjing 210023, P. R. China

Supporting Information

ABSTRACT: Platinum(IV) complexes are prodrugs of cisplatin with multiple potential advantages over platinum(II) drugs. Mitochondria play pivotal roles in producing energy and inducing death of cancer cells. Two platinum(IV) complexes, namely, *c,c,t*-[Pt(NH₃)₂Cl₂(OH)(OCOCH₂CH₂CH₂CH₂PPh₃)]Br and *c,c,t*-[Pt(NH₃)₂Cl₂(OCOCH₂CH₂CH₂CH₂PPh₃)₂]Br₂, were designed to explore the effect of mitochondrion-targeting group(s) on the bioactivity and cytotoxicity of platinum(IV) complexes. The complexes were characterized by electrospray ionization mass spectrometry, reverse-phase high-performance liquid chromatography, and multinuclear (¹H, ¹³C, ³¹P, and ¹⁹⁵Pt) NMR spectroscopy. The introduction of triphenylphosphonium targeting group(s) markedly influences the reactivity and cytotoxicity of the Pt(IV) complexes.

The targeted complex displays more potent disruptive effect on mitochondria but less inhibitory effect on cancer cells than cisplatin. The lipophilicity of the Pt(IV) complexes is enhanced by the targeting group(s), while their reactivity to DNA is decreased. As a result, the mitochondrial morphology and adenosine triphosphate producing ability are impaired, which constitutes an alternative pathway to inhibit cancer cells. This study shows that both the reactivity of platinum(IV) center and the property of axial targeting ligand exert influences on the cytotoxicity of targeted Pt(IV) complexes. For targeting groups with pharmacological activities, their intrinsic function could enrich the anticancer mechanism of Pt(IV) complexes.



INTRODUCTION

Platinum anticancer drugs represent one of the great successes in inorganic medicinal chemistry. These drugs typically modify nuclear DNA (nDNA) by forming bifunctional intrastrand cross-links, triggering inhibition of DNA transcription and apoptosis of cancer cells.¹ Pt(IV) complexes with a kinetically inert d⁶ metal ion center and a six-coordinate octahedral geometry are prodrugs of cisplatin.² They may not only avoid the attack of off-target biological nucleophiles before reaching the purine bases in nDNA but also provide opportunities to tether additional ligands for tumor targeting or drug delivery.^{3,4} These axial ligands could be reduced by ascorbic acid (AsA) or glutathione (GSH) existing preferentially in tumor cells to generate corresponding divalent species.⁵ Therefore, rational choice of axial ligand offers a platform for fine-tuning the pharmacological properties of Pt(IV) scaffold with higher lipophilicity and kinetic inertness.

Mitochondria are principal subcellular organelles responsible for producing adenosine triphosphate (ATP) to provide the energy required by cells.^{6–8} In addition, they regulate the release of proapoptotic factors, such as cytochrome c (Cyt c), and thereby control the intrinsic apoptotic pathway. Apart from apoptosis, other modes of cell death, such as necrosis, necroptosis, and autophagy, are also related to mitochon-

dria.^{9–11} In recent years, mitochondria are recognized as one of the most important targets for anticancer chemotherapy.¹² However, very few structural analogues of cisplatin have been explored for targeting mitochondria and ultimately leading to apoptosis of cancer cells; and the effects of Pt(IV) complexes on mitochondria are largely unexplored.^{13–15} The barrier toward mitochondria is their highly impermeable membrane, which holds a substantial negative potential (200 mV) across it.¹⁶ Currently, an effective way to deliver drugs specifically to mitochondria is to link lipophilic cations such as the triphenylphosphonium (TPP) cation to a pharmacophore of interest.¹⁷ Moreover, TPP-based cations are typically more efficient in inhibiting cancer cell proliferation as compared to other lipophilic cations, and some TPP-linked compounds have been developed to selectively target cancer cells.^{18–20} However, to the best of our knowledge, only one study reported the development of a Pt(IV) complex tethered with TPP to target the mitochondria of cancer cells.²¹

Recently we synthesized two biotin-guided Pt(IV) complexes to target cancer cells and found that the mono-biotinylated complex is superior to the di-biotinylated one.

Received: June 21, 2018

Though tethering two biotin groups to cisplatin enhances more Pt content in cancer cells, the mono-biotinylated one benefits the reaction with DNA and cytotoxicity due to faster reduction than the former. It seems that the monotargeted Pt(IV) complex is more active than the ditargeted one in terms of reactivity and cytotoxicity.²² In this study, we synthesized two mitochondrion-targeted Pt(IV) complexes, namely, *c,c,t*-[Pt(NH₃)₂Cl₂(OCOCH₂CH₂CH₂CH₂PPh₃)(OH)]Br (PMT) and *c,c,t*-[Pt(NH₃)₂Cl₂(OCOCH₂CH₂CH₂CH₂PPh₃)₂]Br₂ (PDT, Figure 1), bearing TPP as a homing moiety for

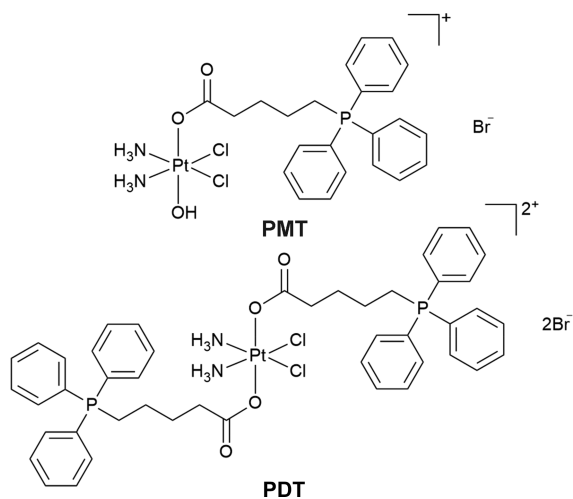


Figure 1. Chemical structures of PMT and PDT.

mitochondria. It was found that TPP has a significant effect on the bioreactivity and cytotoxicity of the Pt(IV) complexes. However, the results are not in accordance with our previous observations. PDT was more efficiently taken up by cancer cells to disrupt the morphology and respiration function of mitochondria; it was more cytotoxic than PMT in inhibiting cancer cells. The results demonstrate that the effect of mitochondrion-targeting group on the cytotoxicity of Pt(IV) complexes is distinct from that of the pure tumor-targeting group.

RESULTS AND DISCUSSION

Synthesis and Characterization. Complexes PMT and PDT were synthesized by reacting oxoplatin and (4-carboxybutyl)triphenylphosphonium bromide (CTPP) in dimethyl sulfoxide (DMSO) solution, respectively (Scheme S1), which were fully characterized by ¹H, ¹³C, ³¹P, ¹⁹⁵Pt NMR, electrospray ionization–mass spectrometry (ESI-MS), and high-resolution mass spectrometry (HR-MS; Figures S1–S4). The purity of PDT was ascertained to be 98% by analytical high-performance liquid chromatography (HPLC; Figure S5). Both PMT and PDT are lipophilic in that they are soluble in a range of organic solvents such as methanol, chloroform, dimethylformamide, and DMSO. Compared with other mitochondrion-targeted platinum complexes,²³ PMT and PDT have the advantage of facile synthesis and simple molecular structure, which allow us to focus on investigating their biological properties.

Cytotoxicity. The *in vitro* cytotoxicities of PMT and PDT were first tested by the frequently used 3-(4,5-dimethylthiazol-2-yl)-2,5-diphenyltetrazolium bromide (MTT) assay in four cell lines, namely, the human non-small cell lung cancer

(A549), the human breast cancer (MCF-7), the human cervical cancer (HeLa), and the human normal liver (L-O2) cell lines. The half maximal inhibitory concentration (IC₅₀) values based on the data of MTT assay are summarized in Figure 2. PMT and PDT only showed mild or moderate

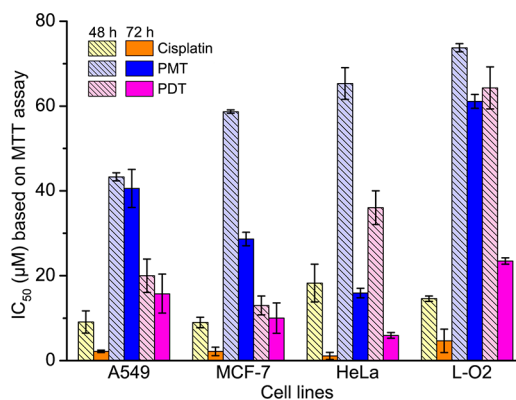


Figure 2. IC₅₀ values (µM) of PMT, PDT, and cisplatin for A549, MCF-7, HeLa cancer cell lines, and L-O2 normal cell line at 48 and 72 h determined by the MTT assay.

cytotoxicity at 48 and 72 h, particularly PMT, while cisplatin displayed a strong activity as usual. The MTT-based IC₅₀ values of PMT and PDT decreased evidently at 72 h as compared with those at 48 h. The time-dependent cytotoxicity suggests that these Pt(IV) complexes need enough time to be reduced or activated into Pt(II) species.

However, since PMT and PDT are supposed to target mitochondria and interfere with mitochondrial functions, while the MTT assay measures mitochondrial dehydrogenase activity as the marker of cell viability,²⁴ so the above results may only reflect the effect of the complexes on the mitochondrial metabolism rather than the viability of the cells. To avoid the possible spurious result, the cytotoxicity was redetermined by the neutral red uptake (NRU) assay, which tests the uptake of neutral red in viable cells and incorporation of the dye in lysosomes, being irrelevant to the mitochondrial metabolism.²⁵ The IC₅₀ values of PMT and PDT based on the NRU assay at 72 h are listed in Table 1. The trend of the cytotoxicity is the same as that observed in the MTT assay; that is, PMT is less cytotoxic than PDT against cancer cell lines, and both are less potent than cisplatin. The axial ligand CTPP is almost nontoxic under the same conditions. The physical mixtures of cisplatin and CTPP (1:1 and 1:2) exhibit cytotoxicities comparable to that of cisplatin, suggesting the released axial ligand(s) barely contribute to the cytotoxicity. The IC₅₀ values of PMT and PDT for the L-O2 cell line are quite high, implying that PMT and PDT are less toxic to normal cells. The NRU-based IC₅₀ values are somewhat lower (~20%) than those of the MTT-based IC₅₀ values, suggesting that mitochondrial metabolism is not the only factor determining the viability of the cells. Interestingly, the cytotoxicity of PDT is higher than that of PMT toward all the tested cell lines, which differs from our previous result that monomodified Pt(IV) complex is more cytotoxic than the dimodified one.²² The difference may result from the nature of targeting group and cellular accumulation of the complexes (*vide infra*).

Lipophilicity and Cellular Uptake. Lipophilicity (log P) is a key property that affects the membrane penetration ability and administration route of a drug.²⁶ We hence tested the log

Table 1. IC₅₀ Values (μM) of PMT and PDT for A549, MCF-7, HeLa Cancer Cell Lines, and L-O2 Normal Cell Line at 72 h Determined by the NRU Assay, with Those of Cisplatin, CTPP, and Their Combinations as References

complex	A549	HeLa	A549	L-O2
PMT	34.30 \pm 3.58	12.29 \pm 0.31	34.30 \pm 3.59	>64
PDT	12.20 \pm 2.29	6.42 \pm 1.03	12.20 \pm 2.29	33.54 \pm 1.74
cisplatin	7.58 \pm 0.93	1.72 \pm 0.10	7.58 \pm 0.93	16.57 \pm 3.72
CTPP	>64	>64	>64	>64
cisplatin + CTPP	9.38 \pm 1.31	2.15 \pm 0.04	9.38 \pm 1.31	36.52 \pm 4.04
cisplatin + 2 CTPP	13.55 \pm 2.38	1.74 \pm 0.41	13.55 \pm 2.38	>64

P of PMT and PDT using the shake-flask method in a 1-octanol/phosphate buffer system (pH 7.4).²⁷ Both complexes are regularly distributed between water and *n*-octanol (Figure S6). On the basis of UV-vis absorbance data (Table S1), the log *P* values for PMT and PDT are calculated to be -0.64 and -0.60 , respectively, showing that they are more lipophilic than cisplatin (log *P* = -2.3).²⁸ The lipophilicity of these complexes follows an order of PDT > PMT > cisplatin, which seems to be positively related to the number of lipophilic CTPP ligand in the complex. Since lipophilicity can enhance the affinity of a platinum compound for the cellular membrane, and cationic compounds could be transported through the organic cation transporters (OCT), PMT and PDT are expected to penetrate the lipid bilayer of cell membrane more easily than cisplatin.

To assess the intracellular accumulation and distribution of PMT and PDT, the Pt content in the membrane, cytosol, nucleus, and cytoskeleton of A549 cells was quantified by inductively coupled plasma-mass spectrometry (ICP-MS) using a cell fractionation kit. The results are shown in Figure 3. Although the total Pt content associated with the cells is

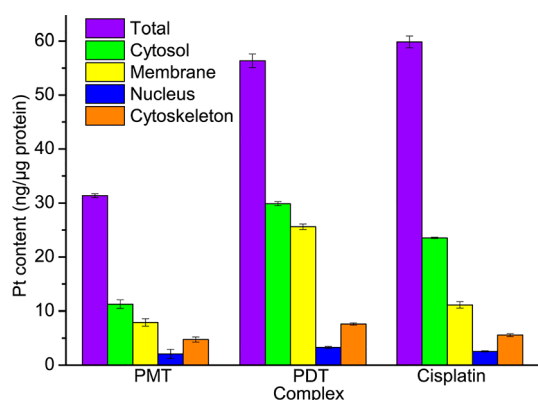


Figure 3. Pt accumulation levels in A549 cells after treatment with 10 μM of PMT, PDT, and cisplatin, respectively, for 24 h.

seemingly high, a considerable amount of Pt is trapped in the cell membrane. The actual cellular Pt accumulation should be the remaining Pt after deducting the stuck part. Therefore, the Pt content inside A549 cells is 23.44, 30.75, and 48.75 ng per μg whole protein for PMT, PDT, and cisplatin, respectively; in other words, the actual Pt content inside A549 cells is just 74.7%, 54.6%, and 81.5% of the total cell-associated Pt for PMT, PDT, and cisplatin, respectively. The results seem to imply that large molecules are easy to be stuck in the cell membrane. However, the results do not correlate with the above lipophilicity (log *P*) of the complexes, in that the most hydrophilic cisplatin has the highest accumulation in cells. This counterintuitive result suggests that lipophilicity is not the only determinant for the cellular uptake; other factors such as

molecular size and electric property also influence the cellular uptake. Nevertheless, the cellular Pt accumulation of these complexes correlates well with the cytotoxicity (Figure 2); for example, PMT has the least cellular accumulation; it shows the lowest cytotoxicity toward the cancer cells. The nuclear Pt accumulation is 2.08 and 3.27 ng per μg whole protein for PMT and PDT, respectively, which cannot account for the big gap between the cytotoxicities of PMT and PDT. The results suggest that some non-nDNA pathway is involved in the cytotoxic action of PMT and PDT.

The Pt content in the mitochondria of A549 cells was also determined by ICP-MS using a mitochondria isolation kit. All the complexes could enter mitochondria with a Pt accumulation of 57.18 \pm 1.56, 21.12 \pm 0.16, and 38.95 \pm 1.32 ng per μg mitochondrial protein for PMT, PDT, and cisplatin, respectively. PMT shows the highest Pt accumulation in mitochondria as compared with PDT and cisplatin. However, since the reduction of PMT is much faster than that of PDT, PMT may enter mitochondria largely in the form of cisplatin, which would not lead to mitochondrial damage (vide infra), being consistent with its lowest cytotoxicity among the three complexes. Because the content of Pt is related to the damage of mitochondrial DNA (mDNA), the results imply that non-mDNA pathway is involved in the cytotoxic mechanism of PMT and PDT.

Reduction Kinetics. The reduction of PMT and PDT by AsA, one of the major reducing agents for Pt(IV) complexes in cells, was monitored by ESI-MS, respectively, at 37 $^{\circ}\text{C}$ in the dark for several days. As shown in Figure 4, the peaks of PMT and PDT at *m/z* 679.17 and 512.25, respectively, weakened gradually, and that of axial ligand CTPP at *m/z* 363.33 grows in the presence of AsA as the reaction time extends. However, the reduction rate is quite different, in that PMT was reduced almost completely after 24 h, while some PDT still existed after 24 h and did not disappear until 3 d later. Although the reduction of PMT is faster than PDT as expected, the cytotoxicity of PMT is much weaker than that of PDT. This inconformity may arise from the relative low cellular Pt accumulation of PMT and non-DNA cytostatic bypath for these complexes (vide supra).

Reactivity and DNA Platination. The reaction of PDT with guanosine-5'-monophosphate (5'-GMP), a model compound of DNA, was studied by ¹H NMR spectrometry at 37 $^{\circ}\text{C}$. The reaction was monitored in the presence of 10 times AsA. Figure 5A displays the NMR spectra in the δ 8.0–8.8 ppm area. The signals at 8.10 and 8.55 ppm are assigned to the H8 of free and N7-Pt(II)-bound GMP, respectively. After incubation for 2 d, the H8 peak of Pt-GMP adduct appears at 8.55 ppm and increases slowly as the time extends. The H8 peak of free GMP is still larger than that of Pt-GMP adduct even after 6 d. The NMR results indicate that the reactivity of PDT with 5'-GMP is very low, which may result from the slow

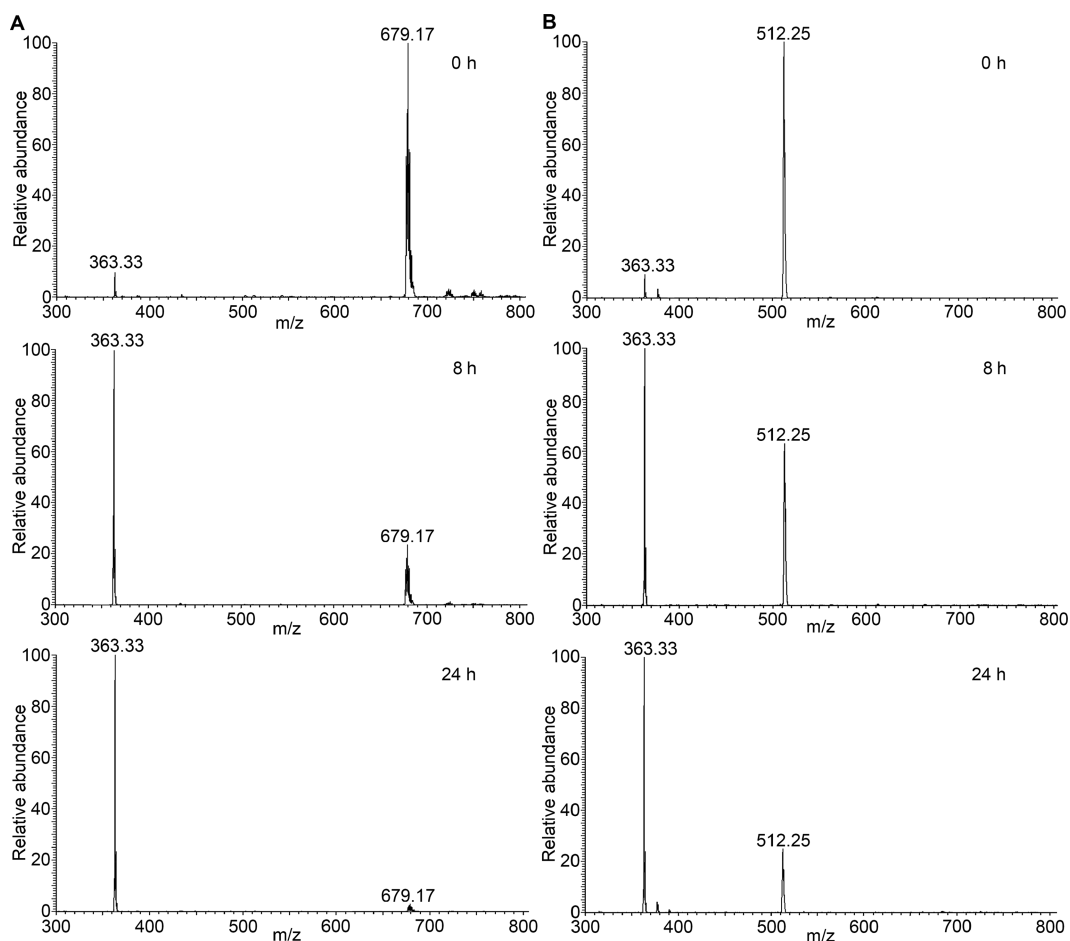


Figure 4. ESI-MS spectra for the reduction of PMT (A) and PDT (B) (2 mM) with 2 equiv of AsA in 70% H₂O/30% CH₃OH solution at 37 °C.

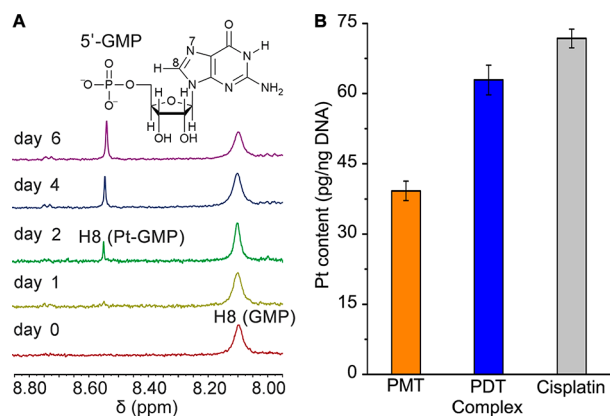


Figure 5. Time-dependent ¹H NMR spectra for the reaction of PDT (1 mM) with 5'-GMP (2 mM) determined in the mixture of AsA (10 mM) and 70% D₂O/30% CD₃OD at 37 °C (A), and platination of cellular DNA (pg Pt/ng DNA) in A549 cells induced by PMT, PDT, and cisplatin (10 μM), respectively, after incubation for 24 h (B).

reduction kinetics of PDT. Further, a DNA isolation reagent (DNAzol) was used to quantify the Pt covalently bound to nDNA in A549 cells. As shown in Figure 5B, although the reduction of PMT is faster than that of PDT, the level of DNA platination induced by PMT is markedly lower than that induced by PDT due to its less cellular accumulation. Cisplatin is the most effective DNA binder among the three complexes. The reactivity of Pt(IV) complexes to DNA is decreased

significantly by the TPP targeting group, which may explain their weaker inhibition to cancer cells. The levels of DNA platination for these complexes are consistent with their cytotoxicity, suggesting that DNA binding still plays a crucial role in the anticancer action.

Apoptosis and Cell Cycle. The pathway to cell death induced by PDT or cisplatin was studied by flow cytometry. A549 cells were treated with the complexes, respectively, for 48 h and stained with Annexin V-FITC (FITC = fluorescein isothiocyanate) and propidium iodide (PI) to evaluate the percentage of live (Annexin V-/PI-), early apoptotic (Annexin V+/PI-), late apoptotic (Annexin V+/PI+), and necrotic (Annexin V-/PI+) cells. As shown in Figure 6, both complexes displayed a capacity to induce apoptosis as compared with the control. PDT, like cisplatin, mainly induced cells to undergo early apoptosis, but the effect was much weaker than that of cisplatin due to the reduction rate of PDT being relatively slow (vide supra). The lower potency just reflects the prodrug nature of Pt(IV) complexes; that is, they need some time to be reduced to active Pt(II) species. These apoptotic results are basically in line with the cytotoxicity data.

The cell cycle of A549 cells was subsequently analyzed by flow cytometry after staining DNA with PI. The cells showed totally different cell cycle distribution characters after treatment with PDT and cisplatin, respectively. PDT arrested the cells mainly in the G1-phase, while cisplatin arrested mainly in the S-phase (Figure S7). The results strongly suggest that the mechanism of antiproliferative action of PDT differs from that

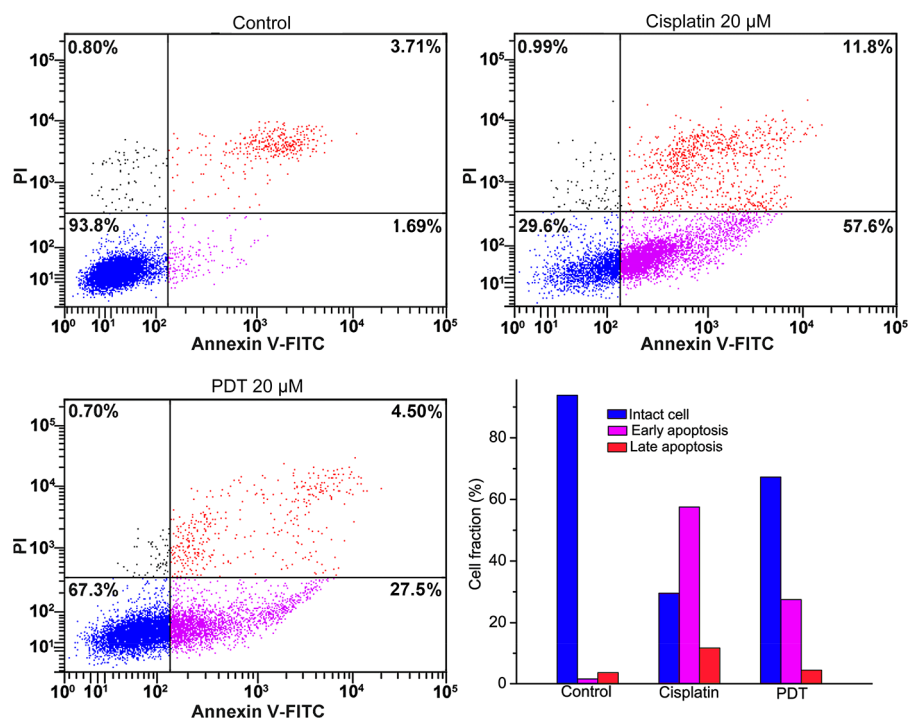


Figure 6. Representative distribution of A549 cells at different stages after incubation with PDT and cisplatin, respectively, for 48 h and staining with Annexin V-FITC and PI. Percentage of A549 cells at each stage was analyzed by flow cytometry.

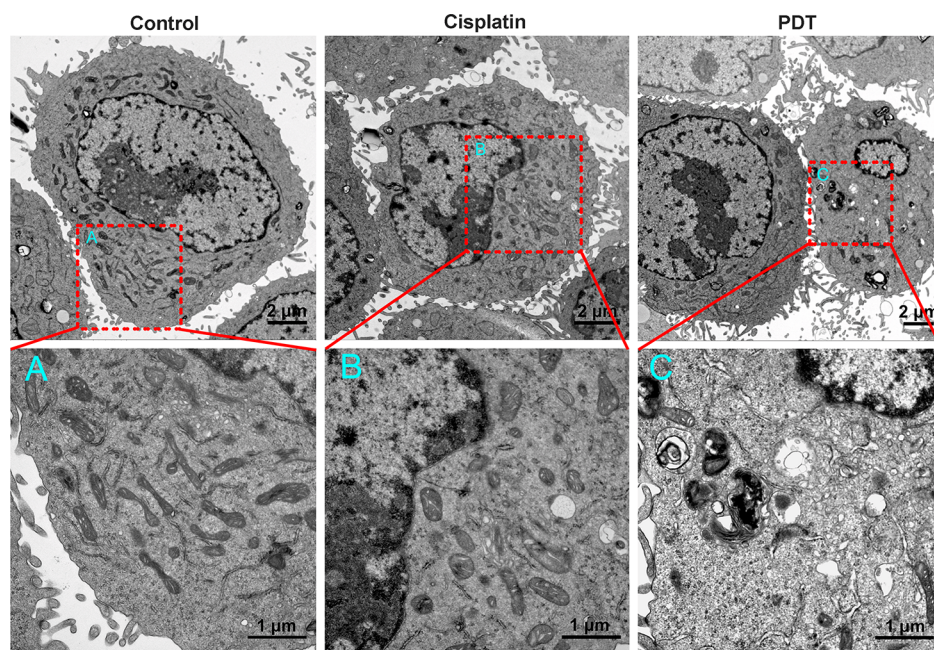


Figure 7. TEM images of mitochondria in A549 cells after treatment with 10 μM of cisplatin and PDT, respectively, for 24 h.

of cisplatin; furthermore, they confirm that cisplatin inhibits cells primarily through disrupting DNA, whereas PDT may affect the cells partially via destroying mitochondria in addition to DNA damage.

Mitochondrial Morphology and Membrane Potential.

Mitochondrion is an organelle constituted by peripheral and inner membranes. Recently, several studies showed that exogenous metal complexes could cause changes in mitochondrial morphology.^{29a} As PMT and PDT can get into mitochondria of A549 cells, we hence chose PDT as a

representative to determine whether it can directly disrupt the morphology of mitochondria. Transmission electron microscopy (TEM) was used to examine the ultrastructure of mitochondria.^{29b} As shown in Figure 7, the mitochondria in untreated A549 cells are identified with typical features, including the well-defined integral double membranes and regular cristae. The mitochondria of cisplatin-treated cells only showed subtle changes in the shape. In contrast, the morphology of mitochondria in PDT-treated cells changed significantly. The structure of most mitochondrial membranes

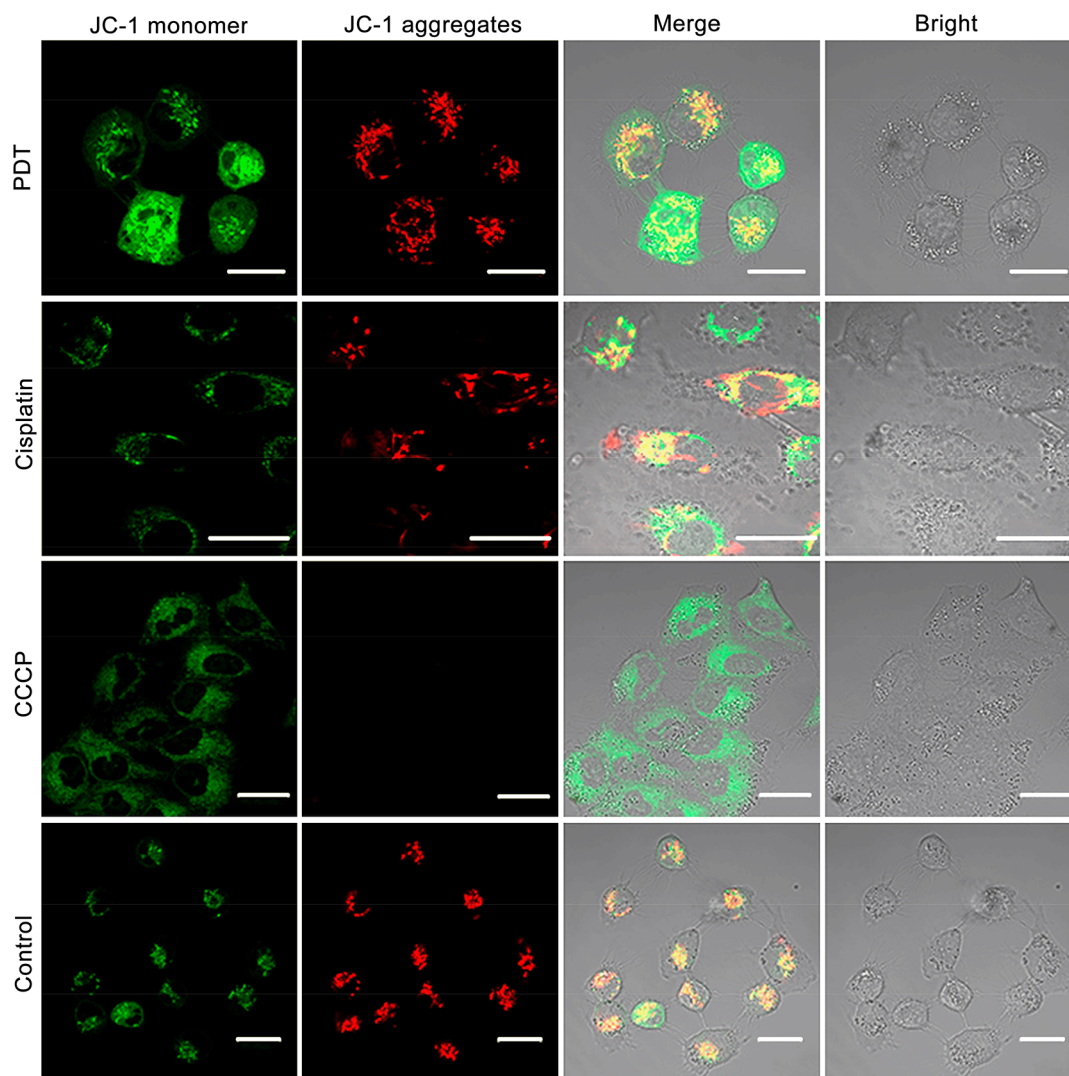


Figure 8. Fluorescence changes of A549 cells after treatment with 10 μM of PDT and cisplatin, respectively, for 24 h and staining by JC-1 dye, with carbonyl cyanide *m*-chlorophenylhydrazone (CCCP, 50 μM , 1 h) as a control for mitochondrial depolarization and collapse of mitochondrial membrane potential. Scale bars: 20 μm .

could not be recognized; some mitochondria were damaged with distortion of cristae and partial or total cristolysis, even forming vacuoles. These observations indicate that PDT can disrupt or damage the mitochondria of cancer cells.

In addition to morphology, mitochondrial membrane potential ($\Delta\Psi_m$) also relates to the capacity of cells to generate ATP by oxidative phosphorylation (OXPHOS).³⁰ Therefore, we detected the $\Delta\Psi_m$ changes by staining A549 cells with 5,5',6,6'-tetrachloro-1,1',3,3'-tetraethyl-imidacarbocyanine iodide (JC-1 dye) after incubation with PDT and cisplatin, respectively, for 24 h. The $\Delta\Psi_m$ in normal cells is high, where JC-1 assembles to form J-aggregates with strong red fluorescence, while in apoptotic or abnormal cells is low, where JC-1 exists as a monomer with green fluorescence.³¹ In Figure 8 the green fluorescence of PDT-treated cells is stronger than that treated by cisplatin or control cells. These phenomena were further confirmed by the quantification of JC-1 fluorescence. The depolarization of mitochondria can be indicated by the increase of "green (G) to red (R)" fluorescence ratio. Quantitative analysis of JC-1-stained A549 cells reveals a big increase in the G (low $\Delta\Psi_m$) to R (high $\Delta\Psi_m$) ratio in PDT-treated cells ($G/R = 2.46$) compared with

control cells ($G/R = 0.28$) or the cells treated with cisplatin ($G/R = 0.84$) at equal Pt concentration. These results confirm that PDT has a greater impact on mitochondrial membrane potential than cisplatin.

Mitochondrial Bioenergetics. The inner membrane of mitochondria contains all the respiratory enzyme complexes that are necessary for OXPHOS, and the mitochondrial respiratory chain generates an electrochemical proton gradient, that is, $\Delta\Psi_m$, which is important for ATP production.³² Thus, the changes of mitochondrial morphology and $\Delta\Psi_m$ are linked to the alteration of metabolic status, especially the OXPHOS process of cells. To ascertain whether PDT can affect mitochondrial bioenergetics, we measured the oxygen consumption rate (OCR) as an indicator of OXPHOS using the Seahorse XF²⁴ Cell Bioanalyzer.³³ As shown in Figure 9A, the OCR of mitochondria decreases significantly as the concentration of PDT increases, which indicates that PDT can inhibit the OXPHOS in A549 cells. Furthermore, we assessed the key energetic parameters reflecting the status of mitochondrial functions, including OCRs for basal respiration, ATP production, and proton leak, respectively. The OCR for basal respiration reduced apparently with the increase of PDT

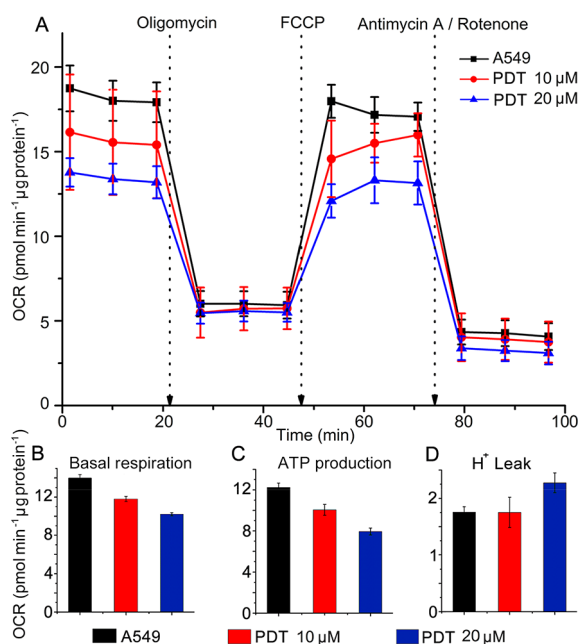


Figure 9. Overall mitochondrial OCR profiles of A549 cells in response to different concentrations of PDT at 18 h (A) and key energy-profiling data involved in the process (B–D). OCR for basal respiration = $OCR_{\text{initial}} - OCR_{\text{antimycin A/rotenone}}$, OCR for ATP production = $OCR_{\text{basal}} - OCR_{\text{oligomycin}}$, OCR for proton leak = $OCR_{\text{oligomycin}} - OCR_{\text{antimycin A/rotenone}}$.

(Figure 9B), indicating that the basal mitochondrial OXPHOS was repressed by this compound. The OCR consumed for making ATP also decreased obviously with the increase of PDT (Figure 9C), suggesting that the ATP producing ability of mitochondria was inhibited. The OCR consumed with passive proton leakage across the mitochondrial inner membrane, which reduces the $\Delta\Psi_m$, slightly increased with the increase of PDT (Figure 9D), implying that the mitochondrial membrane was damaged. These results show that PDT can alter the bioenergetics of mitochondria by suppressing the basal respiration and ATP production of mitochondria and thereby lead to the death of cancer cells.

Glycolysis. The Warburg effect in cancer cells has been widely recognized, which is characterized by a shift of the main source of ATP production from OXPHOS to aerobic glycolysis.³⁵ We therefore determined the effect of PDT on aerobic glycolysis in A549 cells using Seahorse XF²⁴ Cell Bioanalyzer. As shown in Figure 10A, the extracellular acidification rate (ECAR), which approximates glycolytic activity under certain conditions, was dramatically decreased by PDT, indicating that PDT can inhibit the aerobic glycolysis of A549 cells. To further understand the role of PDT in regulating aerobic glycolysis, we analyzed the indices of glycolysis and glycolytic capacity as well as glycolytic reserve. The ECAR response to the adscititious glucose is considered as the basal glycolysis, that is, the rate of glycolysis under basal conditions; the ECAR change after the injection of oligomycin, which inhibits mitochondrial ATP production and hence shifts the energy production to glycolysis, is regarded as the maximum glycolytic capacity of the cells; and the percentage of ECAR variation after oligomycin injection is defined as the glycolytic reserve. As shown in Figure 10B, the basal glycolysis is reduced after the treatment with PDT, corresponding to the suppressed mitochondrial respiration (see Figure 9B). After

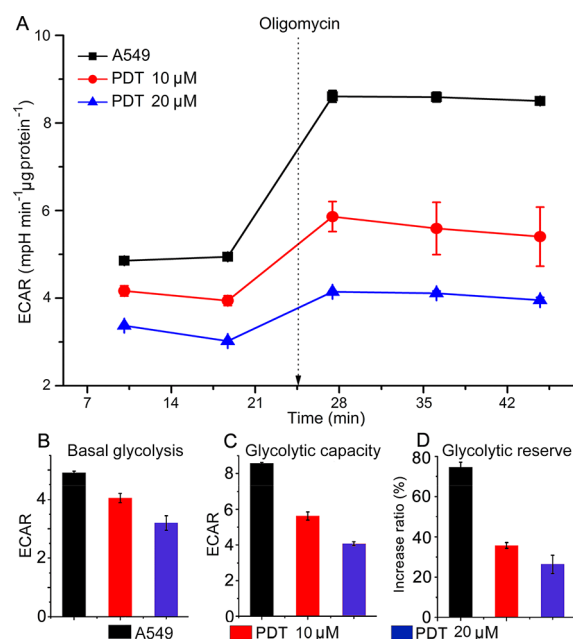


Figure 10. ECAR of A549 cells in response to different concentrations of PDT at 18 h (A), and the calculated parameters for glycolysis (ECARs before oligomycin injection) (B), glycolytic capacity (ECAR after oligomycin injection subtracts baseline) (C), and glycolytic reserve (percentage of ECAR increase after oligomycin injection) (D).

the injection of oligomycin, the glycolytic capacity is significantly weakened by PDT (Figure 10C), and accordingly the cellular glycolytic reserve is reduced by at least 50% (Figure 10D). Our findings suggest that PDT not only inhibits the ATP production of mitochondria but also suppresses the aerobic glycolysis to cut off the energy supply for tumor growth, thus showing an alternative cytostatic pathway for Pt(IV) complexes.

Release of Cytochrome c. Mitochondria play an important part in the apoptosis induced by various triggers. The mitochondrial apoptosis is triggered by the translocation of Bax (a proapoptotic protein) into mitochondria, thereby leading to the release of Cyto c from the mitochondrial intermembrane space to cytosol.³⁶ Therefore, changes in Cyto c in A549 cells was examined to further explore the influence of PDT on the apoptosis induced by the mitochondrial dysfunction. As presented in Figure 11, PDT could lead to a

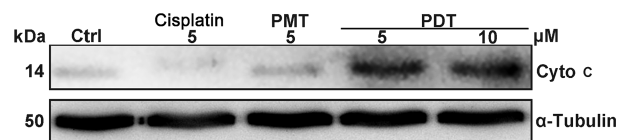


Figure 11. Cyto c expression in A549 cells after treatment with cisplatin, PMT, and PDT (5 μM) for 48 h.

dose-dependent increase in the amount of Cyto c; by contrast, cisplatin barely changed the amount of Cyto c. The increased expression of Cyto c indicates that PDT can promote the release of Cyto c from mitochondria and hence induce the apoptosis of A549 cells through the mitochondria-mediated pathway. The effect of PMT and cisplatin on Cyto c is negligible.

CONCLUSIONS

In summary, two mitochondrion-targeted Pt(IV) complexes, PMT and PDT, were synthesized and investigated. Introducing mitochondrion-targeting group TPP to the axial position of a Pt(IV) complex greatly influences its bioreactivity and cytotoxicity. TPP on one side enhances the lipophilicity of the complex; on the other side it reduces the reactivity of the complex due to the inertness to reduction. Although our targeted complex exhibits stronger disruptive effect on mitochondrial morphology and function than cisplatin, the cytotoxicity is inferior to that of cisplatin. Therefore, Pt(IV) complexes with targeting axial ligands do not necessarily produce superior cytotoxicity in cancer cells. In comparison with our previous biotin-modified Pt(IV) complexes, we found a reverse tendency in cytotoxicity; that is, the monomodified complex (PMT) is less cytotoxic than the dimodified one (PDT). Because of this paradox, we suppose that the cytotoxicity of a targeted Pt(IV) complex may be dependent on both the reduction potential and the nature of targeting group. For pure tumor-targeting groups like biotin, the monomodified complex is more cytotoxic, because it is more readily to be reduced, and its efficacy basically comes from DNA binding; for bioactive targeting groups like TPP, the dimodified complex is more cytotoxic, because in addition to DNA-binding the targeting group per se has pharmacological activity, and two targeting groups would affect tumor cells more effectively than one. With regard to PMT, the reduction would result in the loss of targeting group, giving a Pt(II) species similar to cisplatin, so the targeting group turns out to be an obstacle for the bioactivity. Of course, more evidence is needed to testify this presumption. Anyway, the cytotoxicity of targeted Pt(IV) complexes is related both to the property of axial ligand and to the reactivity of overall complex. For the redox-inert Pt(IV) complexes, the function of axial ligands is particularly crucial for mediating the cytotoxicity toward cancer cells. These findings provide some deeper understanding on the relationship between functional modification and improvement of cytotoxicity in the design of Pt(IV) prodrugs.

EXPERIMENTAL SECTION

Materials and Methods. All reagents and solvents were of analytical grade and used as received without further purification. Cisplatin was purchased from Shandong Boyuan Pharmaceutical Co. Ltd. CTPP, *O*-(benzotriazol-1-yl)-*N,N,N',N'*-tetramethyluronium tetrafluoroborate (TBTU), triethylamine (TEA), *N*-dimethylformamide (DMF), DMSO, hydrogen peroxide (30%), dichloromethane (DCM), sodium sulfate anhydrous, trifluoroacetate (TFA), methanol, diethyl ether, and acetonitrile were purchased from J&K Scientific. 1-Ethyl-3-(3-dimethylaminopropyl)carbodiimide (EDC), *N*-hydroxysuccinimide (NHS), AsA, 5'-GMP, and MTT were purchased from Sigma-Aldrich. Annexin V conjugated with fluorescein isothiocyanate (Annexin V-FITC) and PI were purchased from KeyGen Biotech. Co. Ltd. Mitochondrial membrane potential assay kit (JC-1) was purchased from Biotechnology. Cytochrome c antibody (ab76237) and goat antirabbit HRP (ab97051) were purchased from Abcam. Ultrapure water was prepared using a Millipore Simplicity System (Millipore). IR spectra (KBr pellets) were recorded in the range of 500–4000 cm^{-1} on a Bruker VECTOR22 spectrometer. ESI-MS data were obtained using an LCQ spectrometer (Finnigan). The isotopic distribution patterns for the complexes were simulated using the ISOPRO 3.0 program. HR-MS data were measured on an Agilent 6540Q-TOF HPLC-MS spectrometer. ^1H , ^{13}C , ^{31}P , and ^{195}Pt NMR spectra were acquired on Bruker DRX-400/-500 and Bruker Avance III 600 spectrometers at 298 K. The content of Pt was determined on an ICP-MS using a standard Plasma-Quad II instrument (VG

Elemental, Thermo OptekCorp.). Analytical reversed phase HPLC (RPLC) was conducted on a Shimadzu Prominence using Inertsil ODS-SP column (5 μm , 4.60 \times 250 mm, 1.0 mL min^{-1} flow). Confocal fluorescence imaging studies were performed with a ZEISS Laser Scanning Microscope (Zeiss LSM 710). TEM images were obtained using a JEOL JEM-2100 transmission electron microscope. Flow cytometric analysis was performed by using Cytomics FC500 Flow Cytometry (Beckman Coulter Ltd.). The optical density (OD) of formazan was determined using a Tecan Sunrise ELISA Reader at 570 nm.

Synthesis and Characterization. *Oxoplatin.* Oxoplatin was synthesized in a manner analogous to the literature report.³⁷ Hydrogen peroxide (30 wt %, 20 mL) was added dropwise to the suspension of cisplatin (400 mg, 1.33 mmol) in H_2O (12 mL) at 60 $^\circ\text{C}$. After 4 h, the bright yellow solution was cooled at room temperature overnight to afford yellow crystals. The crystals were filtered and washed with cold water. Yield: 301 mg, 67.8%.

TPP-NHS ester. TPP-NHS was prepared by the addition of EDC-HCl (211 mg, 1.10 mmol) and NHS (127 mg, 1.10 mmol) to the solution of CTPP (433 mg, 1.00 mmol) in acetonitrile (15 mL). After it was stirred at room temperature for 12 h, a colorless solution was obtained. Acetonitrile was removed by rotary evaporation to yield a colorless raw product, which was dissolved in DCM and washed with water three times. Organic layer was collected, and anhydrous Na_2SO_4 was added to remove water. Finally, a white powder was gained by removing the solvent. Yield: 370 mg, 68.52%. ^1H NMR (600 MHz, $\text{DMSO-}d_6$) δ (ppm): 1.50–1.71 (m, 4H, $-\text{CH}_2-\text{CH}_2-$), 2.74 (t, 2H, $-\text{CH}_2-\text{COO}$), 2.79 (t, 4H, $\text{CH}_2-\text{CO}-\text{N}$), 3.35–3.64 (m, 2H, $\text{P}-\text{CH}_2-$), 7.77–7.90 (m, 15H, $\text{P}-\text{Ar}-\text{H}$). ESI-MS (positive mode, m/z) found (calcd) for $[\text{M}-\text{Br}]^+$: 460.42 (460.17).

PMT. PMT was prepared by a published method with some modifications.³⁸ A solution of TPP-NHS ester (194 mg, 0.36 mmol) in anhydrous DMSO (5 mL) was added dropwise to the suspension of oxoplatin (100 mg, 0.30 mmol) in anhydrous DMSO (10 mL) with vigorous stirring. The mixture was stirred at 30 $^\circ\text{C}$ for 72 h. DMSO was removed by addition of excessive diethyl ether. The product was extracted with methanol and washed twice with methanol and ether again and then dried in vacuum as a light yellow solid. Yield: 128 mg, 63.04%. ^1H NMR (600 MHz, $\text{DMSO-}d_6$) δ (ppm): 1.60–1.71 (m, 4H, $-\text{CH}_2-\text{CH}_2-$), 2.21 (t, 2H, $-\text{CH}_2-\text{COO}$), 5–92–6.08 (m, 6H, NH_3), 3.64–3.69 (m, 2H, $\text{P}-\text{CH}_2-$), 7.77–7.90 (m, 15H, $\text{P}-\text{Ar}-\text{H}$). ^{13}C NMR (101 MHz, $\text{DMSO-}d_6$) δ (ppm): 180.51, 134.80, 133.64, 133.54, 130.29, 119.01, 118.16, 35.57, 26.46. ^{31}P NMR (162 MHz, $\text{DMSO-}d_6$) δ (ppm): 23.95, ^{195}Pt NMR (86 MHz, $\text{DMSO-}d_6$) δ (ppm): 1054.43. ESI-MS (positive mode, m/z) found (calcd) for $[\text{M}-\text{Br}]^+$: 679.17 (679.48).

PDT. Oxoplatin (50 mg, 0.15 mmol) was stirred in DMF with CTPP (200 mg, 0.45 mmol), triethylamine (46 mg, 0.45 mmol), and TBTU (144 mg, 0.45 mmol) for 2 d. After filtration, the filtrate was collected, and DMF was removed under high vacuum. Addition of ethanol and water to the residue resulted in the precipitation of desired product.³⁹ The crude product was dissolved in methanol and precipitated with diethyl ether several times to obtain a brown powder. Yield: 45 mg, 25.4%. ^1H NMR (500 MHz, $\text{DMSO-}d_6$) δ (ppm): 1.60–1.71 (m, 4H, $-\text{CH}_2-\text{CH}_2-$), 2.28–2.31 (t, 2H, $-\text{CH}_2-\text{COO}$), 3.59 (m, 2H, $\text{P}-\text{CH}_2-$), 6.50 (m, 6H, NH_3); 7.77–7.90 (m, 15H, $\text{P}-\text{Ar}-\text{H}$). ^{13}C NMR (125 MHz, $\text{DMSO-}d_6$) δ (ppm): 180.25, 134.87, 133.67, 133.54, 130.33, 119.14, 118.00, 34.77, 26.34. ^{31}P NMR (202 MHz, $\text{DMSO-}d_6$) δ (ppm): 23.92. ^{195}Pt NMR (107 MHz, $\text{DMSO-}d_6$) δ (ppm): 1218.86. ESI-MS (positive mode, m/z) found (calcd): $[\text{M}]^{2+}$, 512.33 (511.94); $[\text{M}-\text{H}]^+$, 1023.17 (1023.88). Purity (HPLC): 98% at 267 nm [gradient elution from 10% acetonitrile/water (0.1% TFA) to 100% acetonitrile over 20 min at 0.5 mL min^{-1} with detection at 210 and 270 nm].

Cytotoxicity. The cytotoxicity of PMT, PDT, and cisplatin was tested on A549, MCF-7, HeLa, and L-O2 cell lines. A549 cells were cultivated in RPMI-1640, while other cell lines were cultivated overnight in Dulbecco's Modified Eagle's Medium (DMEM) supplemented with 10% heat-inactivated fetal bovine serum and 100 U mL^{-1} penicillin in an incubator under 5% CO_2 at 37 $^\circ\text{C}$.

1. **MTT Assay.** The cells were plated in the 96-well plates with 2×10^3 cells per well. PMT and PDT were dissolved in DMSO, respectively, and then diluted in culture medium to make the concentration of DMSO lower than 1%. Cisplatin was chosen as a positive reference. Solutions of PMT, PDT, and cisplatin were added into the wells, respectively, and incubated for 48 h. MTT [$20 \mu\text{L}$, 5 mg mL^{-1} , phosphate-buffered saline (PBS)] was added to each well and incubated for 4 h. Final samples were dissolved in DMSO ($150 \mu\text{L}$), and the absorbance of the purple formazan was recorded on an ELISA plate reader at 570 nm. Cell viability rates (%) and IC_{50} values were calculated on the data of three parallel tests.

2. **NRU Assay.** The assay was performed according to the reported procedures.⁴⁰ The cells were seeded at the density of 4×10^3 cells in $100 \mu\text{L}$ media per well in a 96-well plate. The cell number per well was selected according to the density found to display linear growth during 24 h of incubation in pilot studies. The cells were replaced with $200 \mu\text{L}$ of fresh media 24 h after seeding, and graded concentrations of complex were added. After the cells were exposed to the complex for 72 h, the medium was replaced with $20 \mu\text{L}$ of neutral red solution (Neutral red cell proliferation and cytotoxicology assay kit, Beyotime), and the cells were incubated at 37°C for another 3 h to allow the vital dye to be absorbed into lysosomes of the viable uninjured cells. Cell lysis solution ($200 \mu\text{L}$) was then added to the cells after washing with PBS solution three times. The absorbance of the solution was measured at 540 nm, and the reference value at 690 nm was subtracted. Each test was repeated three times, and the survival rate was calculated on the data of parallel tests.

Lipophilicity. Lipophilicity was measured in a 1-octanol/buffer system using the shake-flask method.²⁵ Solutions of PMT and PDT (100 , 150 , and $200 \mu\text{M}$) were prepared in the phosphate buffer (10 mM , $\text{pH } 7.4$) presaturated with 1-octanol. Equal volumes (2.0 mL) of the solution and 1-octanol presaturated with the phosphate buffer were mixed and placed in a thermostatic ($25.0 \pm 0.1^\circ\text{C}$) air-bath orbital shaker at 200 rpm for 4 h. The samples were separated into two phases after centrifugation at 2500 rpm for 15 min. The concentration of the solute in the aqueous phase was determined by spectrophotometry ($\lambda_{\text{max}} = 267 \text{ nm}$). According to the law of mass conservation, the drug concentration of the corresponding 1-octanol phase and the lipo-hydro partition coefficient $P_{o/w}$ ($P_{o/w} = C_o/C_w = A_o/A_w$, A stands for absorbance) were calculated.

Cellular Uptake. A549 cells were seeded in a 6-well plate at a density of 2×10^5 cells/well. After incubation for 24 h, the cells were treated with the complex ($10 \mu\text{M}$) for 24 h. The attached cells were washed twice with PBS (4°C). Cell pellets were collected by centrifugation and then digested with nitric acid ($100 \mu\text{L}$) at 95°C for 2 h, followed by addition of H_2O_2 ($50 \mu\text{L}$) and HCl ($100 \mu\text{L}$) to give a fully homogenized solution. The solution was diluted with water, and Pt content was determined by ICP-MS. The distribution of Pt in cytosol, nucleus, and membrane was determined using a FractionPREP cell fractionation kit from BioVision USA.

Mitochondria and cell nuclei were separated by using a commercially available mitochondria isolation kit for cells (Beyotime Inst. Biotech). Briefly, A549 cells were cultivated with PMT, PDT, and cisplatin ($10 \mu\text{M}$), respectively, in RPMI-1640 medium for 24 h and then incubated in 1 mL of mitochondrial lysing buffer on ice for 10 min. The cell suspension was then homogenized for 30 strokes using a tight pestle on ice. The homogenate was subjected to centrifugation at 600 g for 10 min at 4°C , and nuclei were obtained as a deposition. The supernatant was placed in a fresh tube and centrifuged again at $12\,000 \text{ g}$ for 15 min at 4°C to obtain mitochondrial deposition. HNO_3 ($100 \mu\text{L}$), H_2O_2 ($50 \mu\text{L}$), and HCl ($50 \mu\text{L}$) were added to all fractions and boiled in a water bath at 95°C , until the final volume reached less than $50 \mu\text{L}$. MiliQ water was added to each sample to adjust the volume of solution to 1 mL . The Pt content in the samples was tested by ICP-MS.

Reduction and Reactivity. The samples were prepared by reacting PMT and PDT (2 mM) with 2 equiv of AsA in $70\% \text{ H}_2\text{O}/30\% \text{ CH}_3\text{OH}$ solutions. The time course of the reaction was monitored by ESI-MS after the samples were incubated at 37°C for 0, 8, 24 h, respectively, in the dark.

PDT (2 mM) and 2 equiv of $5'$ -GMP were dissolved in a mixture of $70\% \text{ D}_2\text{O}/30\% \text{ CD}_3\text{OD}$ in an NMR tube. Buffers were not used to avoid side reactions with platinum. D_2O containing 10-fold excess of AsA was added into the NMR tube to reach a final PDT concentration of 1 mM . The status of the reaction was examined by ^1H NMR spectroscopy with a Bruker DPX 300 spectrometer at 37°C and different time points.

DNA Platination. Isolation of genomic DNA of A549 cells was performed using a genomic DNA mini preparation kit (Tiangen Biotech Co., LTD). A549 cells were maintained in culture and grew in 10 cm plates to $\sim 90\%$ confluency before being incubated with each complex ($10 \mu\text{M}$) for 24 h. The amount of DNA was quantified with Nanodrop 1000 at 260 nm , and the Pt level bound to DNA was determined by ICP-MS.

Apoptosis and Cell Cycle. Cell death was analyzed by fluorescence-activated cell sorting (FACS) using Annexin V and PI staining assay. A549 cells were seeded in a 6-well plate at a density of 2×10^5 cells per well and incubated in RPMI-1640 incubation medium (2 mL) and allowed to settle for 24 h. The medium was replaced with the fresh one containing PDT and cisplatin, respectively. After incubation for 48 h, the cells were washed twice with cold PBS, trypsinized, and centrifuged (4000 g , 3 min). The supernatant was discarded, and the cells were resuspended in binding buffer ($500 \mu\text{L}$), stained with Annexin V, and incubated in the dark for 15 min. The cells were treated with PI and analyzed by flow cytometry.

A549 cells were exposed to PDT and cisplatin, respectively, at 37°C under $5\% \text{ CO}_2$ for 24 h, and the culture medium was collected carefully. Trypsin was added to the culture medium, and adherent cells were collected after mild centrifugation. The cells were washed with PBS, fixed in ice-cold ethanol (70%) for 6 h, pelleted by centrifugation, washed again, and stained with PI (1 mg mL^{-1}) in PBS for 30 min at 37°C in the dark. The cell cycle of at least 1×10^4 cells was analyzed using flow cytometry, and the data were analyzed with MFLT32.

Morphology and Membrane Potential of Mitochondria. A549 cells (1×10^6) were treated with $10 \mu\text{M}$ of PDT and cisplatin, respectively, for 24 h. The cell samples were prepared, stained with uranyl acetate and lead citrate, and collected on copper grids. TEM images were taken using the JEOL JEM-2100 transmission electron microscope.

A549 cells were cultured at a density of 1×10^6 cells mL^{-1} and allowed to grow overnight at 37°C . Cells were treated with PDT and cisplatin ($10 \mu\text{M}$), respectively, for 24 h at 37°C . A solution of JC-1 ($10 \mu\text{g mL}^{-1}$ in RPMI-1640) was added and incubated at 37°C for 20 min. The cells were isolated and washed thrice with PBS by centrifugation (1800 rpm for 3 min at 4°C), and images of live cells were taken in phenol red free RPMI-1640 media. The fluorescence of green channel was excited at 488 nm , and the emission was collected between 510 and 545 nm . The fluorescence of red channel was excited at 543 nm , and the emission was collected between 575 and 630 nm . Quantification of fluorescence intensities and corrected total cell fluorescence (CTCF) values were performed using ImageJ. Mitochondrial uncoupling was performed using CCCP ($50 \mu\text{M}$, 1 h) prior to JC-1 assay.

Mitochondrial Bioenergetics. OCR was investigated by using Seahorse XF²⁴ Cell MitoStress Test Kit (Seahorse Bioscience). Prior to the assay, XF sensor cartridges were hydrated. A549 cells were seeded in XF²⁴-well cell culture plates at a density of 4×10^4 cells per well and then incubated for 24 h. The cells were then treated with $20 \mu\text{M}$ PDT or cisplatin for 18 h. The cell culture media were changed, and the plate was incubated at 37°C in a non- CO_2 incubator for 1 h before the measurement. Three baseline measurements of OCR were taken before sequential injection of ATP synthase complex inhibitor oligomycin ($1.0 \mu\text{M}$), ATP synthesis uncoupler trifluorocarbonylcyanide phenylhydrazine (FCCP, $1.0 \mu\text{M}$), and a mixture of antimycin-A ($1.0 \mu\text{M}$, an inhibitor of complex III) and rotenone ($1.0 \mu\text{M}$, an inhibitor that prevents the transfer of electrons from the Fe-S center in complex I to ubiquinone). OCR was determined on a Seahorse XF²⁴ Cell Bioanalyzer (Seahorse

Biosciences). Meanwhile, ECAR was measured. The OCR and ECAR data were normalized to per microgram of protein.

Release of Cytochrome c. A549 cells in 6 cm dishes (Corning) were harvested with 0.25% trypsin and washed with PBS after drug treatment for 48 h. Cell lysis buffer (100 μ L) was added to each sample on the ice. Tumor lysates (40 μ g) were electrophoresed on a 12% sodium dodecyl sulfate–polyacrylamide gel electrophoresis (SDS-PAGE) gel. Proteins were transferred onto poly(vinylidene fluoride) (PVDF) membranes and probed with monoclonal anti-cytochrome c, followed by incubation with peroxidase-labeled goat antirabbit horseradish peroxidase (HRP) secondary antibodies. Western blots were visualized by enhanced chemiluminescence detection system.

■ ASSOCIATED CONTENT

● Supporting Information

The Supporting Information is available free of charge on the ACS Publications website at DOI: [10.1021/acs.inorgchem.8b01707](https://doi.org/10.1021/acs.inorgchem.8b01707).

NMR and ESI-MS spectra of TPP-NHS, PMT, PDT, HR-MS spectra of PDT, RP-HPLC of PDT, UV–vis spectra and UV absorbance data of PMT and PDT, cell cycle of cisplatin and PDT (DOC)

■ AUTHOR INFORMATION

Corresponding Authors

*Phone: +862589684549. Fax: +862583314502. E-mail: boxwxy@nju.edu.cn. (X.W.)

*Phone: +862589684549. Fax: +862583314502. E-mail: zguo@nju.edu.cn. (Z.G.)

*Phone: +862589684549. Fax: +862583314502. E-mail: zhenzhu20170620@nju.edu.cn. (Z.Z.)

ORCID

Zijian Guo: 0000-0003-4986-9308

Xiaoyong Wang: 0000-0002-8338-9773

Notes

The authors declare no competing financial interest.

■ ACKNOWLEDGMENTS

We thank the National Basic Research Program of China (Grant No. 2015CB856300), National Natural Science Foundation of China (Grant Nos. 31570809 and 31700714), and Natural Science Foundation of Jiangsu Province (Grant No. BK20150054).

■ REFERENCES

- (1) Johnstone, T. C.; Suntharalingam, K.; Lippard, S. J. The next generation of platinum drugs: targeted Pt(II) agents, nanoparticle delivery, and Pt(IV) prodrugs. *Chem. Rev.* **2016**, *116*, 3436–3486.
- (2) Basu, U.; Banik, B.; Wen, R.; Pathak, R. K.; Dhar, S. The platin-X series: activation, targeting, and delivery. *Dalton Trans.* **2016**, *45*, 12992–13004.
- (3) Rautio, J.; Kumpulainen, H.; Heimbach, T.; Oliyai, R.; Oh, D.; Järvinen, T.; Savolainen, J. Prodrugs: design and clinical applications. *Nat. Rev. Drug Discovery* **2008**, *7*, 255–270.
- (4) Huttunen, K. M.; Raunio, H.; Rautio, J. Prodrugs—from serendipity to rational design. *Pharmacol. Rev.* **2011**, *63*, 750–771.
- (5) Theiner, S.; Varbanov, H. P.; Galanski, M.; Egger, A. E.; Berger, W.; Heffeter, P.; Keppler, B. K. Comparative in vitro and in vivo pharmacological investigation of platinum(IV) complexes as novel anticancer drug candidates for oral application. *JBIC, J. Biol. Inorg. Chem.* **2015**, *20*, 89–99.

- (6) Milane, L.; Trivedi, M.; Singh, A.; Talekar, M.; Amiji, M. Mitochondrial biology, targets, and drug delivery. *J. Controlled Release* **2015**, *207*, 40–58.

- (7) Szewczyk, A.; Wojtczak, L. Mitochondria as a pharmacological target. *Pharmacol. Rev.* **2002**, *54*, 101–127.

- (8) Zielonka, J.; Joseph, J.; Sikora, A.; Hardy, M.; Ouari, O.; Vasquez-Vivar, J.; Cheng, G.; Lopez, M.; Kalyanaraman, B. Mitochondria-targeted triphenylphosphonium-based compounds: syntheses, mechanisms of action, and therapeutic and diagnostic applications. *Chem. Rev.* **2017**, *117*, 10043–10120.

- (9) Gozuacik, D.; Kimchi, A. Autophagy as a cell death and tumor suppressor mechanism. *Oncogene* **2004**, *23*, 2891–2906.

- (10) Wang, C. X.; Wang, G.; Li, X.; Wang, K.; Fan, J.; Jiang, K.; Guo, Y. M.; Zhang, H. Highly sensitive fluorescence molecular switch for the ratio monitoring of trace change of mitochondrial membrane potential. *Anal. Chem.* **2017**, *89*, 11514–11519.

- (11) Yang, Y. H.; Karakhanova, S.; Hartwig, W.; D'haese, J. G.; Philippov, P. P.; Werner, J.; Bazhin, A. V. Mitochondria and mitochondrial ROS in cancer: novel targets for anticancer therapy. *J. Cell. Physiol.* **2016**, *231*, 2570–2581.

- (12) Fulda, S.; Galluzzi, L.; Kroemer, G. Targeting mitochondria for cancer therapy. *Nat. Rev. Drug Discovery* **2010**, *9*, 447–464.

- (13) Liu, X.; Zhang, L. L.; Xu, X. H.; Hui, L.; Zhang, J. B.; Chen, S. W. Synthesis and anticancer activity of dichloroplatinum(II) complexes of podophyllotoxin. *Bioorg. Med. Chem. Lett.* **2013**, *23*, 3780–3784.

- (14) Sun, T. T.; Guan, X. G.; Zheng, M.; Jing, X. B.; Xie, Z. G. Mitochondria-localized fluorescent BODIPY-platinum conjugate. *ACS Med. Chem. Lett.* **2015**, *6*, 430–433.

- (15) Muhammad, N.; Guo, Z. J. Metal-based anticancer chemotherapeutic agents. *Curr. Opin. Chem. Biol.* **2014**, *19*, 144–153.

- (16) Yamada, Y.; Harashima, H. Mitochondrial drug delivery systems for macromolecule and their therapeutic application to mitochondrial diseases. *Adv. Drug Delivery Rev.* **2008**, *60*, 1439–1462.

- (17) Wang, X. H.; Peng, H. S.; Yang, L.; You, F. T.; Teng, F.; Tang, A. W.; Zhang, F. J.; Li, X. H. Poly-L-lysine assisted synthesis of core-shell nanoparticles and conjugation with triphenylphosphonium to target mitochondria. *J. Mater. Chem. B* **2013**, *1*, 5143–5152.

- (18) Oyewole, A. O.; Birch-Machin, M. A. Mitochondria-targeted antioxidants. *FASEB J.* **2015**, *29*, 4766–4771.

- (19) Lu, P.; Bruno, B. J.; Rabenau, M.; Lim, C. S. Delivery of drugs and macromolecules to the mitochondria for cancer therapy. *J. Controlled Release* **2016**, *240*, 38–51.

- (20) Xu, W.; Zeng, Z. B.; Jiang, J. H.; Chang, Y. T.; Yuan, L. Discerning the chemistry in individual organelles with small-molecule fluorescent probes. *Angew. Chem., Int. Ed.* **2016**, *55*, 13658–13699. *Angew. Chem.* **2016**, *128*, 13858–13902.

- (21) Marrache, S.; Pathak, R. K.; Dhar, S. Detouring of cisplatin to access mitochondrial genome for overcoming resistance. *Proc. Natl. Acad. Sci. U. S. A.* **2014**, *111*, 10444–10449.

- (22) Muhammad, N.; Sadia, N.; Zhu, C. C.; Luo, C.; Guo, Z. J.; Wang, X. Y. Biotin-tagged platinum(IV) complexes as targeted cytostatic agents against breast cancer cells. *Chem. Commun.* **2017**, *53*, 9971–9974.

- (23) Wisnovsky, S. P.; Wilson, J. J.; Radford, R. J.; Pereira, M. P.; Chan, M. R.; Laposa, R. R.; Lippard, S. J.; Kelley, S. O. Targeting mitochondrial DNA with a platinum-based anticancer agent. *Chem. Biol.* **2013**, *20*, 1323–1328.

- (24) Fotakis, G.; Timbrell, J. A. In vitro cytotoxicity assays: Comparison of LDH, neutral red, MTT and protein assay in hepatoma cell lines following exposure to cadmium chloride. *Toxicol. Lett.* **2006**, *160*, 171–177.

- (25) Borenfreund, E.; Puerner, J. A. Toxicity determined in vitro by morphological alterations and neutral red absorption. *Toxicol. Lett.* **1985**, *24*, 119–124.

- (26) Manallack, D. T.; Pranker, R. J.; Yuriev, E.; Oprea, T. I.; Chalmers, D. K. The significance of acid/base properties in drug discovery. *Chem. Soc. Rev.* **2013**, *42*, 485–496.

(27) Reithofer, M. R.; Bytzek, A. K.; Valiahdi, S. M.; Kowol, C. R.; Groessl, M.; Hartinger, C. G.; Jakupec, M. A.; Galanski, M.; Keppler, B. K. Tuning of lipophilicity and cytotoxic potency by structural variation of anticancer platinum(IV) complexes. *J. Inorg. Biochem.* **2011**, *105*, 46–51.

(28) Oldfield, S. P.; Hall, M. D.; Platts, J. A. Calculation of lipophilicity of a large, diverse dataset of anticancer platinum complexes and the relation to cellular uptake. *J. Med. Chem.* **2007**, *50*, 5227–5237.

(29) (a) He, C. Y.; Jiang, S. W.; Jin, H. J.; Chen, S. Z.; Lin, G.; Yao, H.; Wang, X. Y.; Mi, P.; Ji, Z. L.; Lin, Y. C.; Lin, Z. N.; Liu, G. Mitochondrial electron transport chain identified as a novel molecular target of SPIO nanoparticles mediated cancer-specific cytotoxicity. *Biomaterials* **2016**, *83*, 102–114. (b) Ye, R. R.; Tan, C. P.; Lin, Y. N.; Ji, L. N.; Mao, Z. W. A phosphorescent rhenium(I) histone deacetylase inhibitor: mitochondrial targeting and paraptosis induction. *Chem. Commun.* **2015**, *51*, 8353–8356.

(30) Li, C. C.; Wu, T. S.; Huang, C. F.; Jang, L. T.; Liu, Y. T.; You, S. T.; Liou, G. G.; Lee, F. J. S. GTP-binding-defective ARL4D alters mitochondrial morphology and membrane potential. *PLoS One* **2012**, *7*, e43552.

(31) Ramu, V.; Gautam, S.; Garai, A.; Kondaiah, P.; Chakravarty, A. R. Glucose-appended platinum(II)-BODIPY conjugates for targeted photodynamic therapy in red light. *Inorg. Chem.* **2018**, *57*, 1717–1726.

(32) Hu, D. F.; Cao, S. L.; Zhang, G. H.; Xiao, Y. H.; Liu, S. D.; Shang, Y. L. Florfenicol-induced mitochondrial dysfunction suppresses cell proliferation and autophagy in fibroblasts. *Sci. Rep.* **2017**, *7*, 13554.

(33) Nickens, K. P.; Wikstrom, J. D.; Shirihai, O. S.; Patierno, S. R.; Ceryak, S. A bioenergetic profile of non-transformed fibroblasts uncovers a link between death-resistance and enhanced spare respiratory capacity. *Mitochondrion* **2013**, *13*, 662–667.

(34) Zhang, J.; Nuebel, E.; Wisidagama, D. R. R.; Setoguchi, K.; Hong, J. S.; Van Horn, C. M.; Imam, S. S.; Vergnes, L.; Malone, C. S.; Koehler, C. M.; Teitell, M. A. Measuring energy metabolism in cultured cells, including human pluripotent stem cells and differentiated cells. *Nat. Protoc.* **2012**, *7*, 1068–1085.

(35) Porporato, P. E.; Filigheddu, N.; Pedro, J. M. B.; Kroemer, G.; Galluzzi, L. Mitochondrial metabolism and cancer. *Cell Res.* **2018**, *28*, 265–280.

(36) Wang, Z. H.; Yang, H. L. EMMPRIN, SP1 and microRNA-27a mediate physon 8-O- β -glucopyranoside-induced apoptosis in osteosarcoma cells. *Am. J. Cancer Res.* **2016**, *6*, 1331–1344.

(37) Shi, Y.; Liu, S. A.; Kerwood, D. J.; Goodman, J.; Dabrowiak, J. C. Pt(IV) complexes as prodrugs for cisplatin. *J. Inorg. Biochem.* **2012**, *107*, 6–14.

(38) Wang, Z. G.; Xu, Z. F.; Zhu, G. Y. A platinum(IV) anticancer prodrug targeting nucleotide excision repair to overcome cisplatin resistance. *Angew. Chem., Int. Ed.* **2016**, *55*, 15564–15568 *Angew. Chem.* **2016**, *128*, 15793–15797.

(39) Zhang, J. Z.; Bonnitza, P.; Wexselblatt, E.; Klein, A. V.; Najajreh, Y.; Gibson, D.; Hambley, T. W. Facile preparation of mono-, di- and mixed-carboxylato platinum(IV) complexes for versatile anticancer prodrug design. *Chem. - Eur. J.* **2013**, *19*, 1672–1676.

(40) Balachandran, P.; Wei, F.; Lin, R. C.; Khan, I. A.; Pasco, D. S. Structure activity relationships of aristolochic acid analogues: Toxicity in cultured renal epithelial cells. *Kidney Int.* **2005**, *67*, 1797–1805.